DEVELOPMENT OF ACOUSTIC COLOUR TECHNIQUE USING MULTI-FREQUENCY SWATH ACOUSTIC BACKSCATTER

5 authors, including:

Yuri Rzhanov
University of New Hampshire
90 PUBLICATIONS   647 CITATIONS

SEE PROFILE

E. Rinde
Norwegian Institute for Water Research
73 PUBLICATIONS   685 CITATIONS

SEE PROFILE

Colin Brown
National University of Ireland, Galway
48 PUBLICATIONS   1,587 CITATIONS

SEE PROFILE

Some of the authors of this publication are also working on these related projects:

Distribution modelling - errors, uncertainties and the effect of quality and resolution View project

Sand Bank Dynamics View project

DEVELOPMENT OF ACOUSTIC COLOUR TECHNIQUE USING MULTI-FREQUENCY SWATH ACOUSTIC BACKSCATTER

Garret Duffy[a], Yuri Rzhanov[b], Eli Rinde[c], Berit Horvei[d], and Colin Brown[a]

[a]Ryan Institute, National University of Ireland Galway, Galway, IRELAND
[b]Center for Coastal and Ocean Mapping (CCOM), University of New Hampshire, USA
[c]Norsk Institutt for Vannforskning (NIVA), Oslo, NORWAY
[d]Kongsberg Maritime (KM), Horten, NORWAY

Contact author: Garret Duffy, Ryan Institute, National University of Ireland Galway, Galway, IRELAND. Fax : +353 (0)91 750533; E-mail: gpduffy@gmail.com

Abstract: *Swath acoustic data collected by multibeam sonar systems is a recognised tool to efficiently map the bathymetry and texture of large areas of seabed so aiding the definition of benthic habitats. Backscatter data may be spatially classified based on either standard measurements of characteristic acoustic angular response curves (ARCs) or backscatter model parameters (inverted from the ARCs) that depend on seabed physical properties. However, the inverted model parameter of "roughness" is intrinsically linked to the acoustic wavelength; only the roughness spectrum with wavelength less than half of the acoustic wavelength affects the surficial acoustic backscatter. Therefore, inferred surficial texture is intrinsically acoustic frequency-dependent. This research tests the feasibility of using multi-frequency acoustic backscatter to create acoustic classes based on a broadband acoustic response to natural roughness spectra. The goal is to generate more accurate spatial delineation of facies.*
EM2040D (300 kHz (continuous wave (CW) pulse)), EM710 (100 kHz (CW)) and EM302 (30 kHz (CW)) benthic acoustic data were collected simultaneously using Kongsberg Maritime's test vessel, Simrad Echo, within the Ormø–Færder Marine Protected Area in Oslofjorden, Norway. 47 line-km of multi-frequency data were collected resulting in a survey extending 2.9 km by 3.2 km. In addition to the latter overlapping survey lines, 5 non-overlapping, 2.9 km-long cross-lines were acquired to investigate anisotropic backscatter effects; the cross-lines were run perpendicular to bathymetric contours to minimise variation of possible depth-dependent benthic texture within a swath. This paper discusses the results of delineations and compares maps for datasets separately and jointly classified with different frequencies.

Keywords: *acoustic classification, multibeam, multi-frequency*

1. INTRODUCTION

As a mapping tool, multibeam echosounders (MBESs) are used primarily as bathymetric measurement devices. While the amplitude and angular dependence of the backscattered signal, from which the "sounding" is extracted, has long been recognised as a useful indicator of seabed rugosity, and by empirical extension, grain size [1], it is usually seen as being secondary in importance to the primary bathymetric function of MBESs. For vessels equipped with only one (narrowband) MBES, the subordinate ranking of multibeam backscatter data has no practical effect but for vessels equipped with more than one multibeam (or a single broadband MBES as suggested by [2]) where, for the dual purposes of highest bathymetric resolution and minimisation of data storage, usually only the highest resolution multibeam is in operation. Backscatter data from the lower frequency MBES is therefore not collected and, since the dominant seabed roughness, usually parameterised as the roughness spectral strength, w_2, and spectral exponent, γ_2, inferred from the angular dependence of MBES backscatter, is inherently acoustic wavelength dependent [3], we propose that potential roughness information is being lost by this practice. The inclusion of additional frequencies of acoustic backscatter, where possible, has been proposed as having great potential for more accurate seabed classification [2, 4, 5].

The assumption is usually made that the roughness spectrum conforms to a single power law and that γ_2 is a constant (usually -3.0 to -3.5 [1]); this allows inversion for w_2 and, by extension, grain size, to be MBES-frequency independent. However, lander-based studies of seafloor roughness spectra observe that the line of best-fit may be composed of at least two, and up to five, line segments [6] and that acoustic data either side of 150 kHz may be scattered from power laws conforming to different spectral parameters [7]. In addition to the latter theoretical basis, a relationship between frequency-dependent backscatter and sediment type has also been detected in MBES data from the Bay of Fundy giving rise to a suggested utility of multi-frequency MBES backscatter for seabed determination and classification [4]. Another feasibility study took a composite image-based approach to the classification of a small dataset of EM1002, EM3002 and Reson 7125 data in Galway Bay and showed promising results for the distinction between shell hash and maërl using the ISODATA algorithm [8]. There are practical issues for the implementation of multi-frequency MBES seafloor classification, namely the attenuation of high-frequency sound in deeper water and the increased size of lower frequency MBES rendering them impractical for survey launches [4], but setting these aside, this paper will examine the utility of multi-frequency MBES backscatter for more accurate seabed classification.

Kongsberg Maritime's test vessel, *Simrad Echo*, was equipped with an EM2040S, EM710, and EM302 for the survey, carried out over two days within Ormø–Færder Marine Protected Area in Oslofjorden (Fig. 1). MBES acquisition parameters (Table 1), e.g. pulse length, were set manually during data acquisition to eliminate backscatter magnitude changes due to automatic depth-dependent pulse length adjustment [4]. Although the MBESs used are "next generation" echosounders, e.g. capable of transmitting chirped frequency-modulated (FM) pulses [2], they were operated in narrowband, continuous-wave (CW) mode to eliminate any possible backscatter artefacts arising from a broadband acoustic signal. The area was surveyed NW-SE with 100% bottom coverage and then re-surveyed with lines on a perpendicular heading. Under the assumption that seabed type was correlated with slope, the latter lines were run perpendicular to bathymetric contours in order that the assumption of homogeneous seabed within a "patch" of 30 consecutive half-swaths was upheld. Only

backscatter data from the slope-perpendicular NE-SW survey lines will be discussed in this paper.
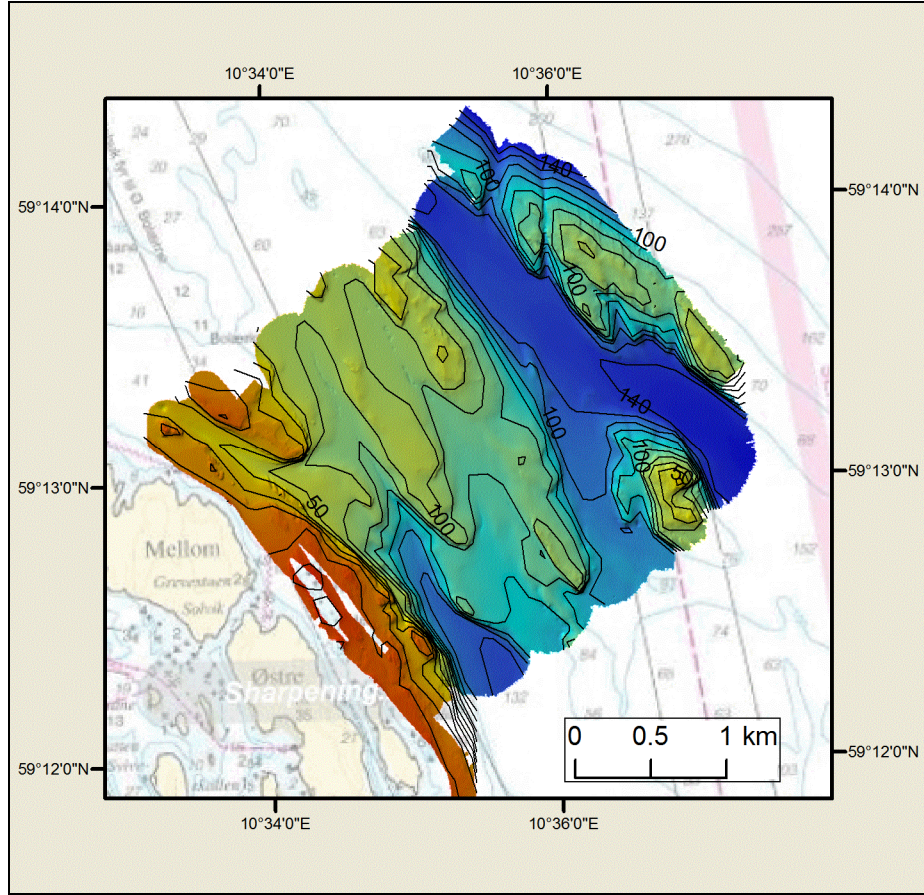

Fig. 1 Five-metre DEM of EM2040 data showing Roche Moutonée, precipitous slopes, and glaciated valleys, topographic features typical of the region.

MBES	Frequency, [kHz]	# Soundings	Transmit x Receive Beamwidth, [°]	Pulse Length (CW), [μs]
EM2040	275, 290, 280 (3 sectors)	400	0.5 x 1.0	600
EM710	71, 83, 77 (3 sectors)	400	0.5 x 1.0	500
EM302	26.5, 30.5, 33.5, 28.5 (4 sectors)	432	2.0 x 2.0	750

Table 1: MBES acquisition parameters.

2. METHODOLOGY

A patch-based approach, whereby angular response curves (ARCs) are averaged in consecutive patches of 30 pings, similar to the approach of Fonseca and Calder [9], was taken with a further modification for spatial joining of co-located patch centroids from the three different frequencies. Using the research version of Geocoder [10], patch-averaged ARCs are decomposed into 5 descriptive parameters: gradient ("x_avo") and intercept (at 10° incidence angle) ("y_avo") of best-fit line to the ARC within the near range (0° to 25°); average AR within the far range (25° to 40°) ("f_avo"); average AR within the near range ("n_avo"); and the fluid factor that is correlated with volume heterogeneities ("ff_avo") [11]. These patch-

based parameters are used as feature vectors for k-means classification but, since the patches corresponding to the different frequency MBES's are independently derived and not co-located, they must be spatially "joined" using conventional GIS software. The Spatial Join process merges the three attribute tables containing the feature vectors for the individual MBESs (Fig. 2 (LEFT)) into one attribute table (Fig. 2 (RIGHT)) so that they can be statistically analysed for clustering and Principal Component Analysis. In practice, the attribute tables of the closest EM710 and EM2040 patch centroids were joined to the EM302 attribute table.
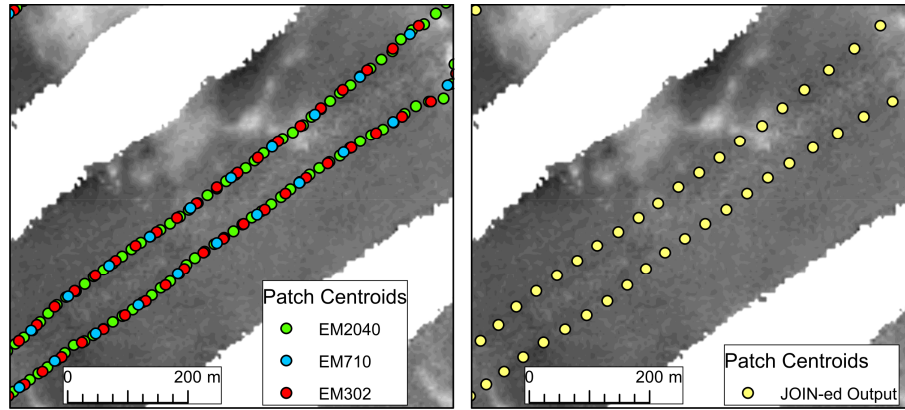

Fig. 2: Port and starboard patch centroids of the different MBESs (LEFT) and (RIGHT) the spatial distribution of the JOIN-ed patch centroids.

K-means cluster analysis and Principal Component Analysis of feature vector attributes were carried out using a Clustering Toolbox [12]. To investigate the effect of different acoustic frequencies on the classification result, the frequency-related feature vectors were classified separately, in pairs (EM2040+EM710; EM2040+EM302; and EM710+EM302), and all together (EM2040+EM710+EM302) to give seven different classification results.
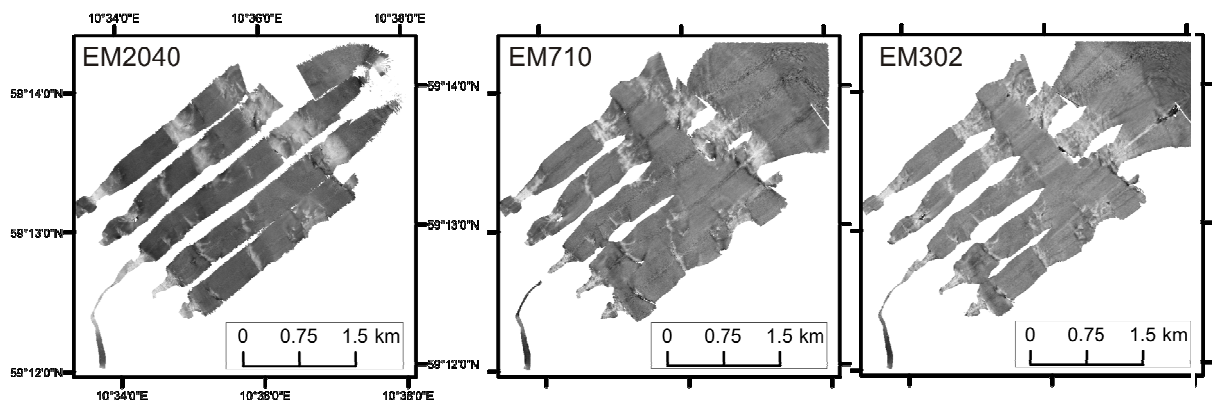
3. RESULTS

3.1. Backscatter Mosaics

Fig. 3: Backscatter mosaics of the MBES cross-lines discussed in this paper.

Time series backscatter data corrections [13] were applied in Geocoder as follows: removal of Lambert's Law correction implemented by the MBES hardware during

acquisition, which assumes a flat seafloor; correction for pulse length dependent footprint area and correction for the actual incident angle using the DEM (Fig. 1). Backscatter data was then mosaicked (Fig. 3).

3.2. K-means Clustering and Principal Components Analysis

Principal Components Analysis (PCA) is suited to testing the discriminatory ability of classifications involving more than one acoustic frequency; ideally, in addition to expected correlation of ARC measurements of the separate ARCs, each frequency will contribute some degree of classification variation along independent orthogonal ("PC") axes. The results of the k-means clustering are displayed in Principal Component space (Fig. 4), where PC1 and PC2, the primary and secondary principal components, are linear combinations of the feature vector attributes (x_avo, y_avo, f_avo, n_avo, and ff_avo) of the patch centroids of one or more of the MBESs used in this study. The cluster centres for classifications including the EM2040 feature vectors (Fig. 4(a, b, c, and g) exhibit a preferred elongation along the PC1 axis and the Eigenvalue of the second principal component is less significant compared to the classifications of the EM710 and EM302 data. This indicates that covariation in the EM2040 and EM710 feature vectors explains the majority of clustering and there is minimal orthogonally distributed, i.e. PC2-orientated, data.
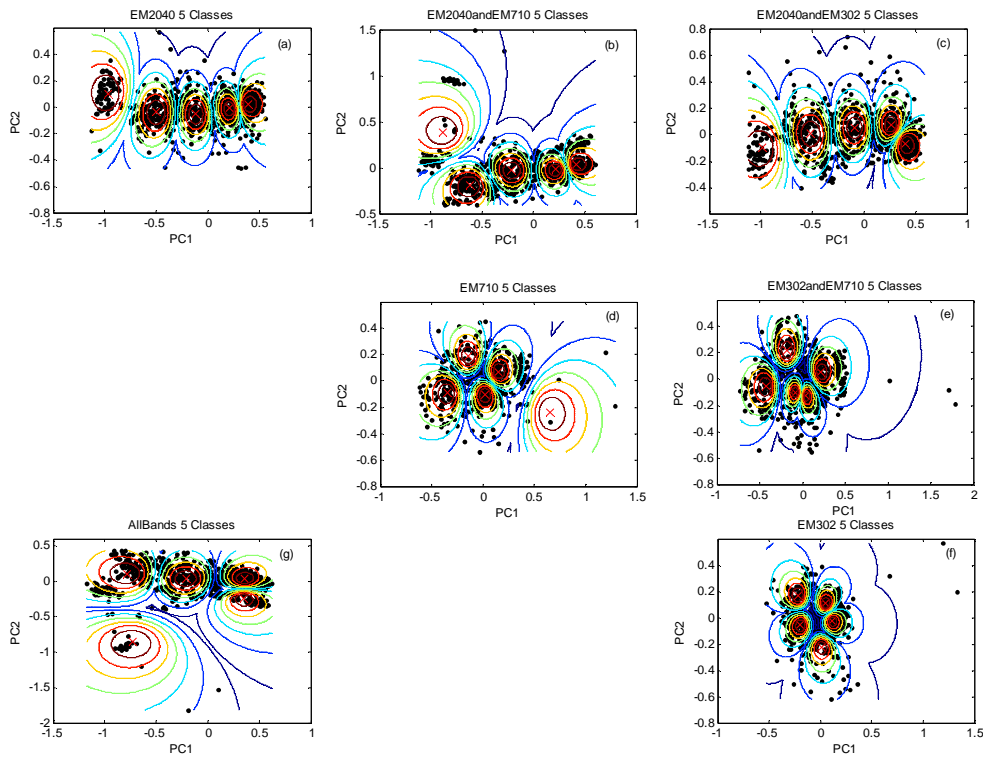

Fig. 4: K-means cluster centres (red crosses) displayed in Principal Component space with contours of Cartesian distance between data point and nearest cluster centre. Eigenvalues, indicating the significance of the component, are bracketed after the axis title.
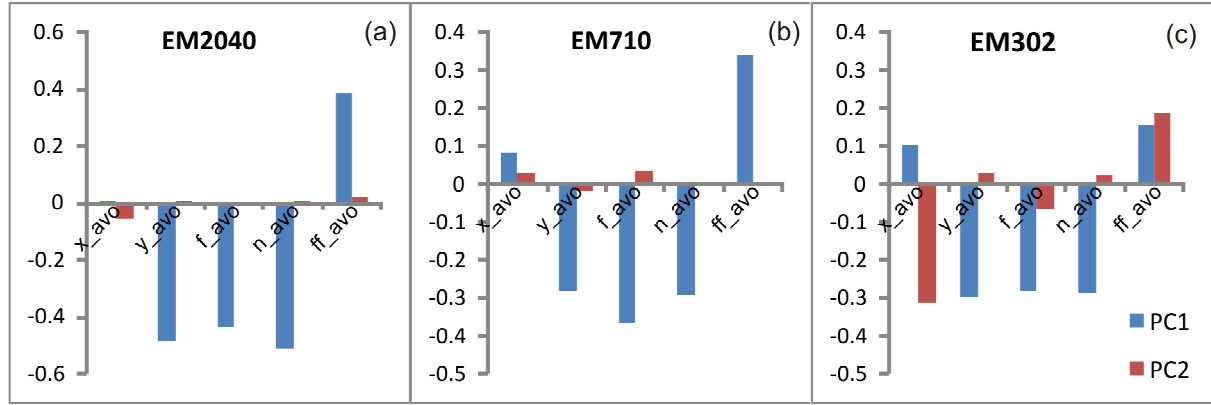
Fig. 5: Eigenvector co-efficients of individual classification of the EM2040 and EM710 feature vectors scaled by the respective eigenvalues.

The main descriptive ARC parameters for the first principal component of the EM2040 are the backscatter value at 10° incident angle, the mean backscatter values in the near and far angular ranges, and the Fluid Factor (Fig. 5(a)). The latter is also true for the EM710 with the addition of a weak dependence on the variation of the slope of the ARC in the nadir region (Fig. 5(b)). By contrast the EM302 exhibits is less discriminatory ability, with classes distributed more isotropically in principal component space (Fig. 4(f)) and the first two principal components are less distinct with eigenvalues of 0.5 and 0.4 respectively.

The power of combining the separate discriminatory characteristics of the EM2040 and EM710 is evidenced by an additional degree of classification freedom for the joint EM2040+EM710 classification (Fig. 6). While the EM710 ARC measurements clearly contribute to the first principal component of variation, indicating unsurprising correlation between the EM2040 and EM710 angular responses, the second principal component is notably strongly dependent on the EM710 ARC measurements alone (red bars, Fig. 6). This indicates that the EM710 is contributing additional discriminatory ability to the joint EM2040+EM710 classification.
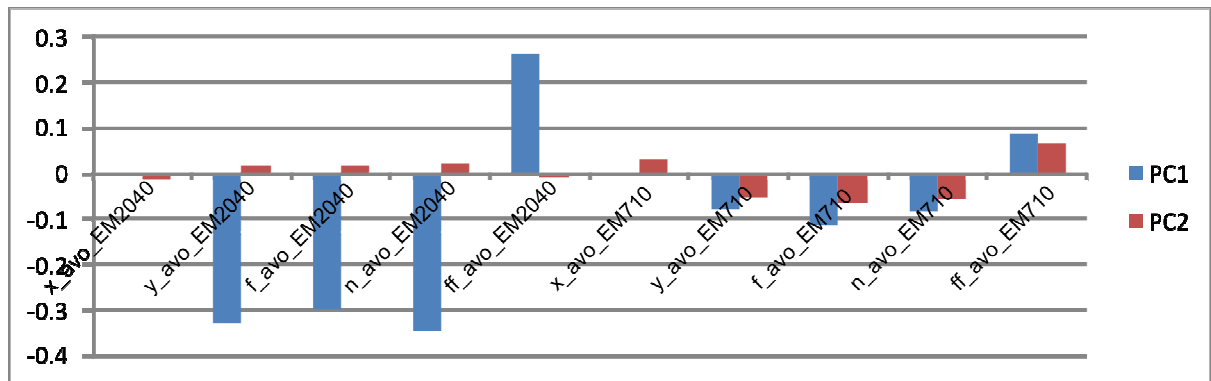

Fig. 6: Eigenvector co-efficients of combined classification of the EM2040 and EM710 feature vectors scaled by the respective eigenvalues. Note the addition of the EM710 introduces a more significant second principal component

3.3. Classification Maps

The results of the k-means clustering were mapped geographically using Voronoi polygons centred on the patch centroids (Fig. 7(g)). Assuming that the sediment types are in reality contiguous and correlated with bathymetry and/or slope, it can be seen that, in the absence of any other information, the classifications involving the EM710 are the most plausible, i.e. EM710 alone (Fig. 7(d)); EM2040+EM710 (Fig. 7(b));and EM2040+EM710+EM302 (Fig. 7(g)). The classification of EM710 alone is quite similar to the classification utilising all three MBES ARC parameters but the latter displays an arguably more realistic distribution of classes four and five and rocky classes one and three are spatially more distinct (Fig. 8). However, the latter remark requires testing by detailed grab sampling, something not carried out to date.

Fig. 7(f) shows that the EM302 is a poor discriminator of the fine sediment within the deep, bifurcating submerged glaciated valley and the fine sediment on the broad flank to the west. However, the addition of EM302 ARC information to the joint classification of EM2040+EM710 Fig. 7(b) leads to better classification of the rocky substrate in the south-western strait Fig. 7(g) and more plausible classification of class five in the southern extremity of Fig. 7(g).

Therefore the classification based on the ARC parameters of all three MBESs may be viewed as a "fine-tuning" of the EM710 (alone) classification.
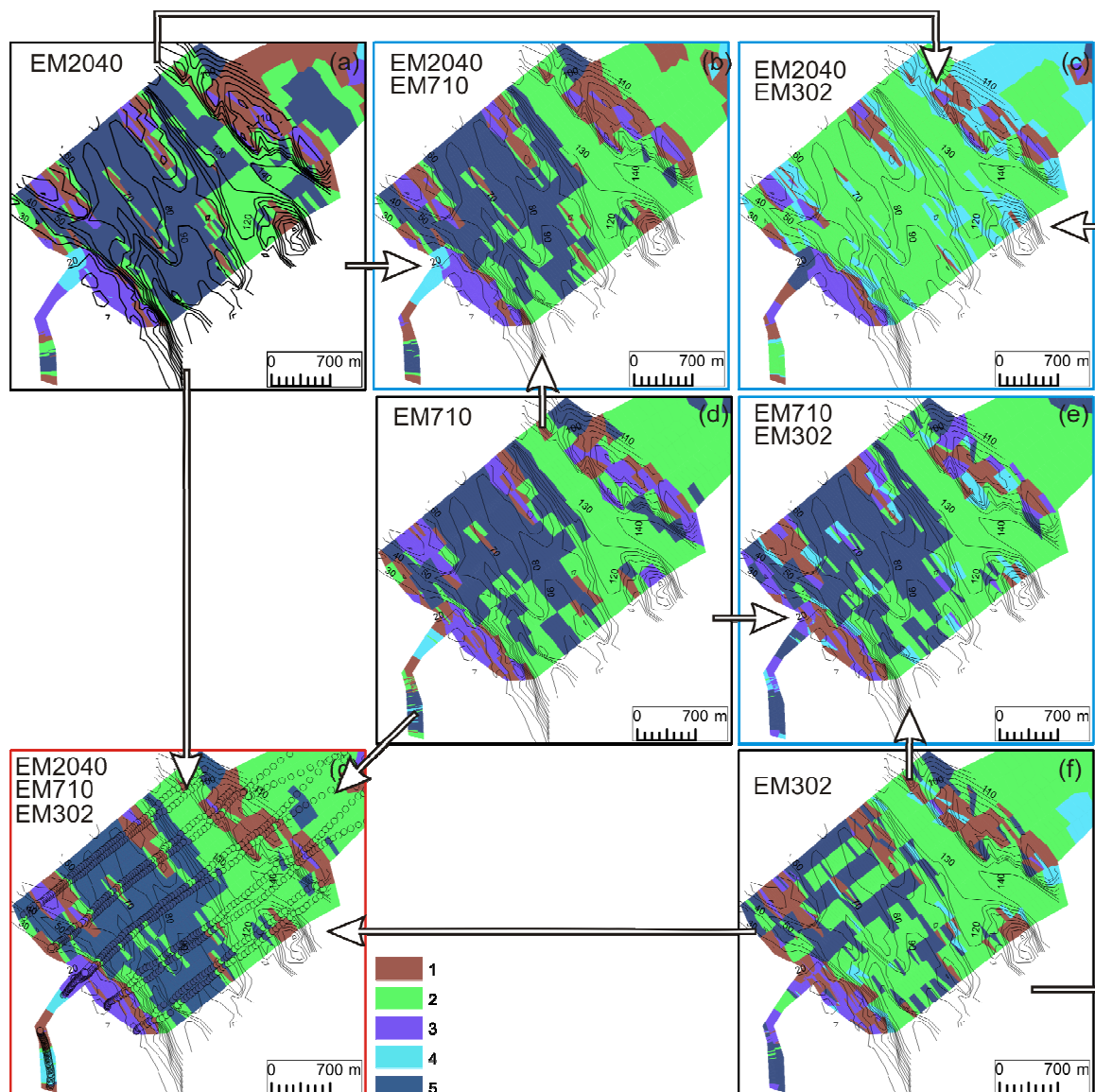
Fig. 7 Classifications based on k-means clustering of ARC measured parameters for: individual MBES (Black outline); jointly classified MBESs (blue); and all three MBESs (red). Bathymetric contours are displayed in metres and patch centroid locations symbolised in (g)
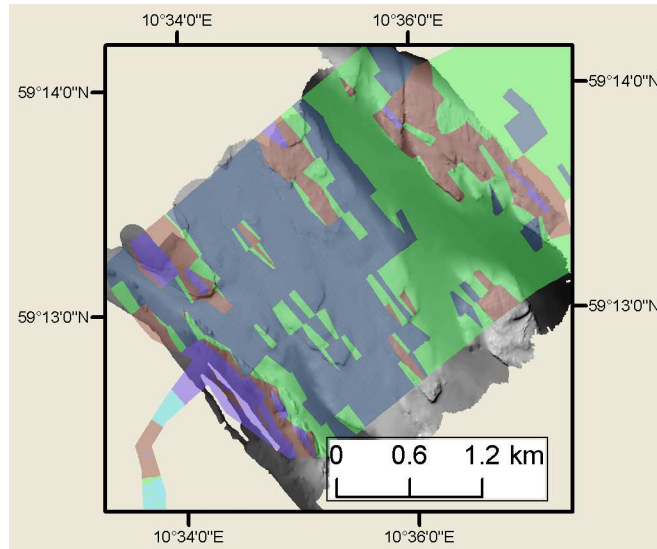
Fig. 8 K-means classes for combined ARC parameters for all three MBESs overlayed on greyscale shaded bathymetry. Purple and brown classes are correlated with rocky seabed morphology, possibly distinguished by thickness of sediment cover.

4. CONCLUSION

This study has tested the feasibility of utilising backscatter from different frequency MBESs for more accurate seabed classification has shown that:

- In the absence of ground-truthing and assuming seafloor type is locally homogenous and related to bathymetry and/or slope, the classification using the EM710 alone produces a plausible regional seafloor configuration
- The inclusion of ARC information from EM2040 and EM302 may be viewed as a "fine-tuning" of the EM710 classification with two more distinctive rocky classes, that, we speculate, may be distinguished by thickness of sediment cover, and better definition of Class 5 sediment in the southern extremity of the field area.

Future work will utilise the entire dataset, i.e. inclusive of the NW-SE survey lines, investigate the use of more ARC descriptive parameters, and utilise other clustering approaches.

REFERENCES

[1]. **Jackson, D.R., D.P. Winebrenner, and A. Ishimaru,** Application of the composite roughness model to high-frequency bottom backscattering. *The Journal of the Acoustical Society of America*, 79(5): p. 1410-1422, 1986.

[2].   **Mayer, L.A.,** Frontiers in seafloor mapping and visualization. *Marine Geophysical Researches*, 27(1): p. 7-17, 2006.

[3].   **Ogilvy, J.,** *Theory of wave scattering from random rough surfaces*. 1991: Taylor & Francis. 292.

[4].   **Hughes Clarke, J.E., et al.** *Inter-calibrating multi-source, multi-platform backscatter data sets to assist in compiling regional sediment type maps : Bay of Fundy*. in *CHC2008*. 2008.

[5].   **Anderson, J.T., et al.,** Acoustic seabed classification: current practice and future directions. *ICES Journal of Marine Science: Journal du Conseil*, 65(6): p. 1004-1011, 2008.

[6].   **Briggs, K.B., D. Tang, and K.L. Williams,** Characterization of interface roughness of rippled sand off fort Walton Beach, Florida. *IEEE Journal of Oceanic Engineering*, 27(3): p. 505-514, 2002.

[7].   **Williams, K.L., et al.,** Acoustic backscattering experiments in a well characterized sand sediment: Data/model comparisons using sediment fluid and Biot models. *IEEE Journal of Oceanic Engineering*, 27(3): p. 376-387, 2002.

[8].   **Duffy, G.P., D. Toal, and F. Stapleton**, *Application of multi-frequency backscatter to seabed determination*, in *GEOSCIENCE 2010*2010: Dublin Castle.

[9].   **Fonseca, L. and B. Calder**. *Clustering acoustic backscatter in the angular response space*. 2007.

[10].   **Fonseca, L. and B. Calder**. *Geocoder: An Efficient Backscatter Map Constructor*. in *Proceedings of the US Hydrographic Conference*. 2005.

[11].   **Fonseca, L. and L. Mayer,** Remote estimation of surficial seafloor properties through the application Angular Range Analysis to multibeam sonar data. *Marine Geophysical Researches*, 28(2): p. 119-126, 2007.

[12].   **Balasko, B., J. Abonyi, and B. Feil,** *Fuzzy Clustering and Data Analysis Toolbox*, in *MATLAB Central File Exchange*, 2005.

[13].   **Hammerstad, E.,** *EM Technical Note: Backscattering and Seabed Image Reflectivity*, 2000, Kongsberg.